ISSN: 2643-6876

Current Trends in Civil & Structural Engineering

DOI: 10.33552/CTCSE.2026.12.000779

Iris Publishers

Review Article

Development of Probabilistic Cracking Models for Fiber Reinforced Concrete Under Static and Dynamic Loadings

Pierre Rossi*

Civil Engineering Department, COPPE, Federal University of Rio de Janeiro, Brazil

***Corresponding author:** Pierre Rossi, Civil Engineering Department, COPPE, Federal University of Rio de Janeiro, Brazil

Received Date: January 27, 2026

Published Date: February 16, 2026

Abstract

This article presents the fundamentals of a numerical model that is set to undergo subsequent algorithmic implementation. This model is a probabilistic semi-explicit cracking model dedicated to the dynamic behavior of structures made from steel fiber reinforced concrete (SFRC). It is based on the extension of the same model that has been previously proposed for static loading. This extension is presented after a detailed exploration of the physical mechanisms accompanying the cracking process of fiber-reinforced concrete under dynamic loading. The fact that the model is based on precise and detailed physical mechanisms allows to propose new theoretical relations concerning strain rate effect on the numerical model parameters. So, an interesting and innovative alternative to the experimental quantification of the model parameters is proposed. This alternative allows to avoid performing tests on sophisticated testing machine as, for example, the Hopkinson bar. It involves conducting only static uniaxial tensile tests on notched fiber-reinforced concrete specimens, that is a fully new and original proposal.

Keywords: Fiber reinforced concrete; dynamic behavior; cracking; finite elements; probabilistic model

Introduction

Dynamic loadings, as considered here, are what are referred to as impulsive-type loadings, caused, for example, by impacts or explosions. It is often emphasized that FRCs (Fiber Reinforced Concretes) perform particularly well under such impulsive loadings. The orders of magnitude of stress and strain rates generated by impulsive loadings in conventional civil engineering structures typically range from 10^{-2} to 10^{3} GPa·s^{-1}, which corresponds to strain rates ranging from 10^{-3} to 10 s^{-1}. Numerous experimental studies on this mechanical issue have shown a clear increase in energy dissipation (non-linear behavior) and load-bearing capacity in structural elements made with FRCs, compared to the same elements made with plain (non-fibered) concrete.

Using fiber reinforced concretes in constructions therefore becomes an important issue when it is known that climate change is now leading to these constructions being subjected to increasingly violent impacts.

To evaluate the specific performance of FRCs under dynamic conditions (i.e., compared to their static performance), it is relevant to analyze whether, for a given mechanical property, denoted as P, the ratio P_{FRC}/P_{CWF} (CWF: Concrete Without Fibers) increases as the stress rate increases, and what physical mechanisms govern the evolution of this ratio.

What follows is a description of the physical mechanisms specific to the behavior of fibers when an FRC is subjected to high strain rates.

In a composite material such as FRCs, sensitivity to strain rate effects can stem from the matrix (concrete), and/or the reinforcement (steel fibers). It is known that, within the aforementioned range of strain rates, steel is much less sensitive to rate effects than concrete. Therefore, in a first approximation, the rate effects in FRCs can be attributed to those of the concrete. These are now well understood [1] and are recalled in chapter 2.

Based on the description of the mechanisms of rate effects within FRCs (Chapter 4), the basis of a numerical model for analyzing the cracking of FRC constructions in dynamic is proposed. This numerical model is founded on the extension of the probabilistic semi-explicit cracking model proposed for static loadings [2].

Strain rate effects on the Tensile Behavior of plain (non-fibered) Concretes

One of the main findings from research conducted to date on strain rate effects is that, within a certain range of strain rates, these effects are primarily linked to the presence of evaporable water within the nanopores of the concrete's hydrates.

A hypothesis has been proposed regarding the physical mechanism in which this evaporable water plays the central role. It is a mechanism akin to the Stefan effect, involving the viscosity of water [1]. This effect can be summarized as follows: when a thin film of a viscous liquid is trapped between two perfectly flat plates that are being pulled apart at a certain velocity, the film exerts a restoring force on the plates that is proportional to the separation velocity.

This mechanism is expressed by the following relationship (1):

$$F = \left(3\eta V^2 / 2\pi h^5\right) \times \left(dh/dt\right) \quad (1)$$

Where:

F is the restoring force,

η, the viscosity of the liquid,

h, the initial distance between the two plates, (dh/dt), the displacement rate of the two plates (> 0), V, the volume of the liquid.

If it is assumed that the free water present in the hydrates is responsible for a similar mechanism when the solid skeleton (here considered as a network of plates) undergoes tensile deformation, we can understand why rate effects are significant in wet concrete. Of course, this Stefan effect should be considered as an explanatory model to aid understanding, and not as a quantitative approach to the rate effect. To understand how the viscous mechanism, similar to the Stefan effect, can influence the tensile fracturing process, one must start from the quasi-static tensile cracking process in concrete.

Tensile cracking process in plain concretes

The cracking process proceeds as follows [3]:

Step 1: Formation and propagation of diffuse microcracking.

Microcracks are small cracks relative to the stressed volume of material. At this scale, they do not cause strain localization. During this initial phase – characterized solely by the formation of microcracks throughout the specimen – the overall behavior appears linear elastic.

Step 2: Transition phase or onset of microcrack localization.

In this phase, some microcracks grow to form mesocracks. These mesocracks induce stress concentrations at different locations within the stressed material, but strain localization at the specimen level has not yet occurred. This is a brief phase in tensile concrete cracking, shifting from microcrack formation to crack propagation. It is associated with the emergence of the nonlinear portion of concrete's tensile response, reflecting its low ductility.

Step 3: Localization of cracking.

This shortest phase in the tensile cracking process begins at the end of step 2. During mesocrack development, one crack begins to dominate, leading to a macrocrack. This signals strain localization at the specimen scale and marks the end of the intrinsic uniaxial tensile behavior of concrete. The concrete's tensile strength is reached at this point.

Step 4: Macrocrack propagation.

This phase concerns the structural behavior of the specimen. Beyond this point, strain localization prevents defining a statistically homogeneous volume of material from mechanical stand- point. The primary mechanical relation becomes the link between the macroscopic tensile force and displacement. During this stage, a reduction in force with increasing displacement is observed when the test is conducted at a fixed displacement rate, illustrating the structural softening behavior (the specimen being considering as a small structural element).

Importance of the Stefan effect on the tensile cracking process of plain concretes

Before localization (steps 1, 2, and 3), the viscous mechanism can have two consequences:

- Delaying the formation of microcracks,
- Delaying the propagation of initial microcracks.

These two actions lead to a delay in the localization of microcracking and thus increase the peak load (So, the uniaxial tensile strength). After localization (step 4), the viscous mechanism (Stefan effect), by acting on the microcracks of the process zone at the front tip of the macrocrack, oppose the propagation of this macrocrack (increase of the macrocrack propagation energy). In parallel with the activation of the viscous mechanism, inertia forces can no longer be neglected when the stress and strain rates generated by dynamic loading reach high values. These inertia forces can influence the cracking process in two different ways before the localization phase under dynamic loading: They oppose both the appearance and the propagation of microcracks, thereby delaying their localization. They also act after the localization phase, by resisting the propagation of the macrocrack.

It is clear that, although they may act simultaneously, the viscous mechanism and the inertia forces are not activated with the same intensity depending on the imposed loading rate. Thus, for strain rates below a critical rate around 1 s^{-1}, inertia forces are negligible compared to viscous effects. However, for strain rates equal to or greater than this value, inertia forces become non-negligible and even dominant for strain rates around 10 s^{-1}. It turns out that if the experimental curve relating tensile strength to strain rate is considered, it deviates from linearity (a sudden increase in strength is observed) for strain rates near 1 s^{-1}.

According to the definitions given regarding material-scale and structural-scale behavior, it is plausible that inertia forces triggered by macrocrack propagation (i.e., after localization) are sufficient, within a certain strain rate range, to generate an increase in the material's tensile strength. In other words, the presence of inertia

forces means that the peak load may not coincide with the onset of crack localization, and thus the observed jump in tensile strength at a strain rate of about 1 s^{-1} could be a structural effect. Based on the dynamic cracking process in concrete, it can be analyzed how steel fibers intervene in this process. To do so, it must first be examined how fibers act in the quasi-static cracking process.

Role of fibers in the tensile cracking process of FRC in static

Fibers' role in the static cracking process can be summarized as follows [3]:

- In steps 1, 2, and 3, fibers can bridge micro- and meso-cracks, delaying the formation of a macrocrack. This improves the material's tensile strength and ductility.
- In step 4, fibers bridge the macrocrack itself, opposing its propagation and increasing the energy required for crack growth. This step is related to a structural behavior (the specimen can be considered, mechanically, as a mini structural element)

This paper does not delve into the specifics of how these bridging effects are achieved, such as fiber type, geometry, dosage, and orientation. For example, bridging effects in steps 1 to 3 can occur in UHPFRC (Ultra-High Performance Fiber Reinforced Concrete) when the fiber content is high (with small diameters) and fibers are well-oriented relative to the crack, usually obtained through uniaxial tensile testing or very high fiber volume fractions (exceeding 5%).

Role of fibers in the tensile cracking process of FRCs under dynamic loading

To influence the dynamic tensile cracking process, fibers must activate additional physical mechanisms compared to the static regime (chapter 3).

Two potential beneficial mechanisms are highlighted:

- Waves diffraction by fibers.
- Synergistic coupling between fibers and concrete.

Waves Diffraction by Fibers

Under impulsive loading, mechanical waves propagate through the material. The wave diffraction by an inclusion (such as a fiber) depends mainly on:

- The contrast in elastic properties and density between the cement paste and the steel fiber,
- The ratio between the wave length and the fiber's length or diameter.

If the period of the wave is compatible with the dimensions of the steel fibers, diffraction is significant due to large contrasts:

- Young's modulus ratio ≈ 10.
- Density ratio ≈ 3.5.

In contrast, aggregates present lower contrasts (modulus ≈ 2.5, density ≈ 1), making them less significant for diffraction. For diffraction to occur, the wavelength λ must be less than about 10 times the fiber length (L), or diameter (Ø). The wave propagation formula to be considered is the following:

$$\lambda = C \times T \qquad (2)$$

(where λ is wavelength, C is wave speed, T is period).

If a long fiber with a length of 60 mm and a short fiber with a diameter of 0.2 mm are considered, it is found that:

- For Ø = 0.2 mm → $T \leq 0.5 \times 10^{-5}$ s
- For L = 60 mm → $T \leq 1.5 \times 10^{-4}$ s

As example, in an experimental study [4] related to impact resistance of concrete slabs (slabs 8 cm thick) subjected to shock tube testing, the following quantitative data were obtained:

- Generated strain rates ≈ 1 s^{-1}
- Natural period of the slab in bending ≈ 2.5×10^{-3} s

This is 1–2 orders of magnitude above the critical diffraction periods, suggesting fibers do not significantly diffract waves during the stationary wave regime. However, wave propagation involves both transient and stationary regimes. During the transient regime, shorter wave periods may occur, comparable to those needed for fiber diffraction. Thus, fibers may indeed diffract mechanical waves early in the process, potentially increasing the volume of material subjected to motion and promoting multiple cracking (which is favorable for fiber efficiency). So, in conclusion, for structures susceptible to cracking during the transient wave regime, wave diffraction by fibers could prevent brittle failure by promoting distributed cracking. This structural effect depends on boundary conditions, loading type, and geometry. Fiber effectiveness increases with volume fraction. However, this mechanism is very hard to model using macroscopic models and would require micromechanical modeling, which is beyond this study's scope.

Synergistic coupling between concrete and steel fibers

In chapter 3, fibers were shown to oppose displacement across crack faces and transfer stresses (bridging effect). Under impulsive loading, crack lips move at high velocity, and fibers are rapidly engaged. In transferring stress, fibers induce high strain rates in the surrounding matrix. Depending on fiber geometry and anchorage, these can be shear, tensile, or compressive stresses. For bond-based fibers, the transmitted stress is macroscopic shear. However, due to surface roughness and matrix heterogeneity, these become tensile stresses at the micro-scale, causing microcracking around the fiber, leading to nonlinear interface behavior. This microcracking near the fiber/matrix interface activates rate effects (as discussed in chapter 2), increasing macroscopic bond strength under dynamic vs. static loading. For mechanically anchored fibers (with hooks at their ends, as example), similar tensile stress concentrations arise, often greater than with bonded fibers. Rate effects here are localized near anchor points, increasing fiber effectiveness before pull-out.

In conclusion, both bonded and mechanically anchored fibers transmit higher forces dynamically than statically, for the same crack width (assuming fibers do not rupture). Thus, whether fibers increase intrinsic strength (as in UHPFRC) or post-crack energy (any FRC), the strength ratio $K_R = R_{FRCs}/R_{Plain}$ or energy ratio $K_E = E_{FRCs}/E_{Plain}$ increases under dynamic loading. This effect scales with fiber volume.

Numerical model of the cracking of FRC concrete structures in static

Existing diffuse cracking models

These models [5–11] treat cracks as microcracked zones where the density of microcracks gradually increases until forming a void, at which point no further stress is transmitted. From a numerical perspective, within the framework of finite element theory, these microcracked zones are modeled using volume elements. Generally, these models follow a deterministic approach and describe the nonlinear mechanical behavior associated with microcracking. The nonlinear mechanical behavior of these elements is linked to the post-peak tensile behavior of Fiber-Reinforced Concrete (FRC). This post-peak behavior is typically characterized by two key material parameters:

- The shape of the post-peak response referring to the behavior of the tensile stress- strain curve after the linear elastic phase of the FRC.
- The post-peak energy dissipation which corresponds to the area under the tensile stress-strain curve and is often referred to as G_f .

In summary, diffuse cracking models applied to FRC rely on nonlinear finite element methods using volume elements. The nonlinear behavior considered is the tensile response of the FRC, represented as a stress-strain relationship. These models consider that the post-peak behavior is the evolution of the microcracking process in presence of fibers. This highlights a major limitation of these diffuse cracking models: they are not physically based if chapters 3 and 4 are considered.

Although these models are widely described in the literature and commonly used in practice, they have a significant drawback. As previously mentioned, diffuse cracking models are not physically based since they transform a localized crack into diffused microcracked zone. This strong physical approximation results in an inaccurate representation of the cracking pattern in FRC structures. Numerically, because G_f values are significantly higher for FRCs than for conventional concretes, diffuse cracking models tend to overly spread the damaged (microcracked) zones and underestimate crack openings.

The most well-known diffuse cracking models for FRC include damage models [5–7] and smeared crack models [8,9], which are mechanically equivalent. Notably, the smeared crack model developed at École Polytechnique de Montréal (Canada) [10, 11] provides a more accurate evaluation of crack openings in FRC compared to other diffuse cracking models. This improvement is attributed to its use of an explicit resolution algorithm, whereas other models employ implicit resolution algorithms. The explicit approach allows for better crack localization. However, despite this advancement, even the smeared crack model has limitations in accurately evaluating crack openings.

The probabilistic semi-explicit cracking (PSEC^f) model for FRC in static

The PSEC^f model for simulating the mechanical behavior of large-scale FRC structures was previously presented for static problems [2]. This PSEC^f model is designed to simulate macrocrack propagation, specifically addressing cracks with openings equal to or greater than 300 microns. It is based on the uniaxial tensile behavior of FRCs. It concerns only FRCs which have softening post-cracking behavior in uniaxial tension. This uniaxial tensile behavior.

The main objective of this model is to address a key limitation in existing distributed cracking models from the literature, namely, the excessive dispersion of cracks, which results in underestimating the openings of major cracks. Macrocrack initiation and propagation are simulated using linear volumetric elements, where cracks form when the tensile stress at the integration point of an element reaches the matrix's tensile strength (unreinforced concrete), assuming perfectly brittle matrix behavior. Concrete strength is modeled as a random variable following a Weibull distribution, with dependence on the finite element volume. As the finite element volume increases, both the mean and standard deviation of the matrix tensile strength decrease.

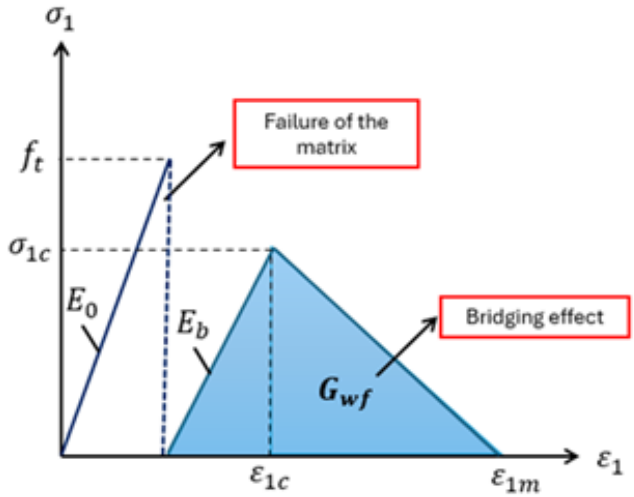

Figure 1: Aspects of the PSEC^f model for fiber-reinforced concrete – Mechanical behavior in uniaxial tension.

As demonstrated in [12], using linear volume elements does not precisely capture macrocrack initiation. However, in the case of fiber-reinforced concrete (FRC), this approximation is acceptable provided that the fiber bridging effect is properly incorporated into the numerical model. Previous experimental study [13] has shown that the average post-cracking energy related to the bridging effect is independent of the tested material volume, although the standard deviation of this energy decreases with increasing volume. Aligning with the objectives of this model, a simplified approach is adopted where the fiber bridging energy G_{wf} is treated as a deterministic parameter, unaffected by the finite element volume. The probabilistic semi-explicit model considers two key mechanical stages: initial macrocrack initiation (step 3 of chapter 2.2) and fiber bridging effect. These aspects are illustrated in Figure 1.

Crack initiation occurs when the maximum principal stress σ_1 in an element reaches the randomly assigned tensile strength f_t. At this point, the element's stiffness decreases sharply. During fiber bridging, as the maximum principal strain ε_1 increases, the bridging mechanism is activated, which increases the effective stiffness E_b but remains below the original material stiffness E_0. If ε_1 decreases, the element's stiffness remains low. During crack progression, once ε_1 reaches a critical value ε_{1C}, the stress σ_1 decreases linearly with ε_1 to simulate fiber pullout. When ε_1 attains its maximum value ε_{1m}, the fiber effect is considered negligible, and the element stiffness drops to zero.

This softening behavior is modeled via a simple damage approach, where only the matrix values in the element related to the maximum principal stress-strain relationship are modified, while other matrix entries remain zero. Consequently, the fiber bridging effect is treated as anisotropic. Given the probabilistic nature of the model, Monte Carlo procedure is essential to ensure the results statistically reflect the variability inherent in both model parameters and material properties. For a given structural problem, the set of obtained results allows for a relevant statistical analysis, enabling a safety-oriented assessment of the structure's behavior.

It can be emphasized that, in the proposed model, the rupture of the matrix (the concrete) being perfectly brittle and its tensile strength a probabilistic parameter, this allows the cracks to be located much better than in the diffuse cracking models mentioned previously.

It is important to clarify that the proposed model is not valid for FRCs which have hardening behavior in uniaxial tension. In this model, the bridging effect of the fibers is only considered when the matrix is fully cracked. This choice might appear overly simplistic given the macroscopic behavior observed during a direct tensile test on a notched specimen. Indeed, during such a test, a softening behavior emerges, resulting from the propagation of the macrocrack and the progressive bridging action of the fibers until the entire section of the specimen is fully cracked. However, as de- scribed in Section 2.1, this macrocrack propagation phase is by no means a material behavior, but rather a structural behavior. In fact, this post-cracking softening behavior entirely depends on the dimensions of the direct tensile specimen, and more specifically on the cross-section where the cracking occurs (in the case of a notched specimen).

As a result, the only stages of the cracking process of fiber-reinforced concrete under direct tension are considered in the model: (1) the behavior up to the initiation of the macrocrack (peak load) which is the material behavior of the uncracked FRC; and (2) the load transfer by the fibers when the specimen's cross-section is fully cracked (which is the material behavior of the fully cracked FRC). Indeed, for the latter stage, it has been experimentally demonstrated [13] that the average behavior of the load transfer by the fibers is independent of the specimen's dimensions. The scattering related to this fibers load transfer behavior decreasing with the in- creasing specimen dimensions, it is important to adapt the number of specimens to be tested to get a correct information about the average behavior [13]. To conclude, all models that incorporate the macrocrack propagation phase into the material behavior model are physically and mechanically incorrect.

Parameters determination of the PSEC^f in static

The mean tensile strength of the matrix ft and its standard deviation (which depends on the finite element volume) are computed from previously validated formulas [14]. These properties are randomly distributed across the mesh following a Weibull distribution. The fiber bond energy G_{wf} is derived from uniaxial tensile test on notched specimens [15,16]. Since this uniaxial tensile test measure crack opening, a conversion to strain is necessary for modeling and numerical simulations. This conversion involves dividing the crack opening by a characteristic length of the finite elements, $l_e = V_e^{(1/3)}$, where Ve represents the volume of the finite element.

An example of test set-up related to the direct tensile test on notched specimen is presented in following. This test set-up has long been validated [3,15,16].

A very good technical solution is to use, as connection between the specimen and the testing machine, aluminum cylinders having the same diameter than the specimen tested. Aluminum having a Young modulus/Poisson ratio close to that of concrete, stress concentration in the glue (which serves to connect the specimen to the aluminum bar) and in the specimen near the connection is very low. These aluminum cylinders are directly screwed on the testing machine. A schematic draw of this test set-up is presented in Figure 2. To minimize this stress concentration, the length of the aluminum cylinders is chosen in relation with the length of the dimensions of the specimen. This length optimization of the aluminum cylinders is made by performing linear finite element analysis (considering both the specimen and the aluminum cylinders).

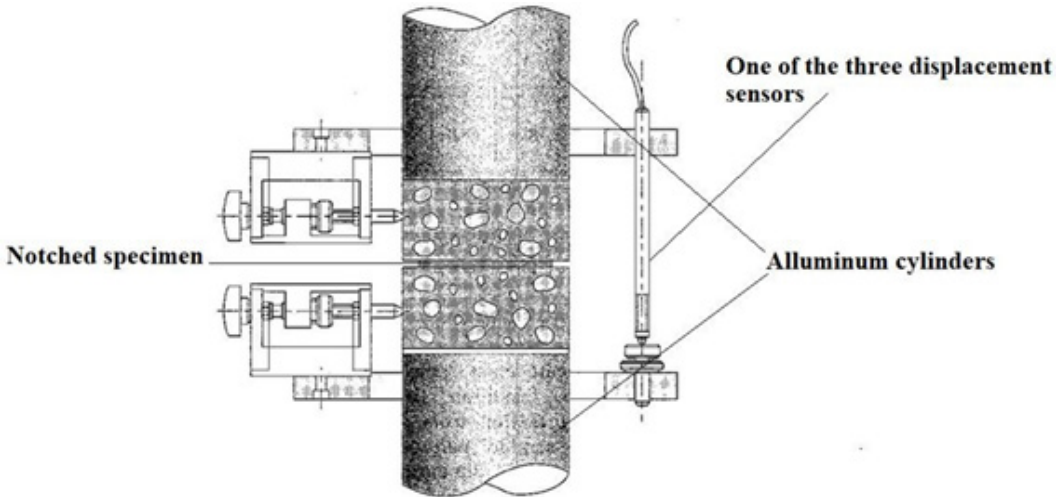

Figure 2: Schematic draw of the bond between the notched specimen and the aluminum cylinders – vertical cut (from [3]).

Determination of the tensile stress-crack opening curve useful to calculate G_{wf}

As précised before, when a notched specimen is concerned, the beginning of the test is related to a macrocrack propagation along the specimen section (at the level of the notch). This propagation coincides with a local bending inside the cracked section. This bending can occur until the complete macrocrack creation. Therefore, the part of the tensile stress-crack opening curve related to this step of crack propagation has not to be considered. The crack is considered completely open along the section of the specimen when all displacement sensors indicate an opening displacement, w0, equal to 10^{-4}. L_s . L_s is the basis length of measurement of the sensors and 10^{-4} corresponds to a conventional value of cracking strain of concrete. After the step of crack propagation, the local bending is less if the test is well performed, whether with the gripping or the bonding connection.

Only when w_0 is reached for all displacement sensors, an average crack opening can be considered. The smaller average crack opening is called w_i . Figure 3 illustrates how w_0 and w_i are determined (case of bounding connection). Consequently, G_{wf} is calculated considering the experimental stress-crack opening curve from the crack opening w_i. It means that for crack openings inferior to wi the fibers bridging effect is not considered. This approximation leads to a conservative numerical simulation with respect to the actual behavior of the structure under consideration.

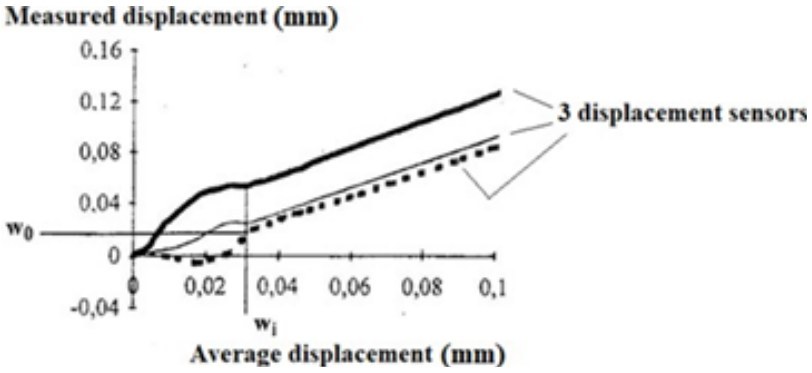

Figure 3: Example of determination of w_0 and w_i (from [3]).

In practice, a number of uniaxial tests need to be conducted to determine the average value of G_{wf} to be used in the numerical simulations.

Determination of ε_{1c}, σ_{1c} and ε_{1m}

σ_{1c} is determined directly from the experimental average tensile stress-crack opening curve. It is the maximal average value of the post-cracking tensile strength.

Concerning ε_{1c} , it is more complicated. The fiber bridging effect being only considered from an experimental crack opening equal to w_i , while, in the numerical model, this bridging effect begins at zero crack opening, it is clear that the value of w_{1c} (and so of ε_{1c}) in the model (w_{1cn}) has to be lower than that observed in the experiment (w_{1ce}). This value of w_{1c} can be calculated considering this point: the experimental bridging effect attributable to a material behavior starts when the volume of the macrocracks is equal to $(w_i.S_p)$, where S_p is the cracked section of the specimen, while the numerical bridging effect starts when the volume element is fully cracked (its rigidity matrix is equal to 0). To get an equivalent bridging effect between the numerical model and the experiment, the following relation as to be considered (as approximation):

$$w_{1cn} = w_{1ce}\left(\left(w_i \cdot S_p\right)/V_e\right) \qquad (3)$$

is calculated as following:

$$\varepsilon_{1m} = 2\,G_{wf} / \sigma_{1c} + \varepsilon_0 \qquad (4)$$

Numerical Model of the SFRC Structures behavior under Dynamic Loading

The majority of numerical models (finite elements models) related to the dynamic behavior of fiber-reinforced concrete structures [17–22] exhibit the same issues as those concerning the static behavior of these structures (chapter 5.1). They are not very relevant for providing a realistic representation of the cracking process (cracking is too diffuse compared to reality). This is due to the same inherent limitations of these models (chapter 5.1).

The proposed model is based on the development in dynamics of the PSEC^f model developed in statics (chapter 5.2). In this PSEC^f model, two parameters appear: the tensile strength f_t of concrete and the bridging effect energy of fibers G_{wf}. Chapters 2, 3, and 4 show that the rate effect on fiber-reinforced concretes have two main consequences: the increase, with the stain rate, of f_t , which is a probabilistic parameter and of G_{wf} which is a deterministic parameter.

Regarding the strain rate effect on ft, significant experimental studies [1] led to the following generic relationship [23]:

$$f_{t,dyn} = f_{t,sat} + 2.8 + 0.3In(\dot{\sigma}) \qquad (5)$$

with strength ($f_{t,sat}$ and $f_{t,dyn}$) given in MPa, while stress rate has units of GPa/s. $f_{t,sat}$ and $f_{t,dyn}$ are respectively the static and the dynamic tensile strengths.

As for the strain rate effect on G_{wf} , there is no generic relationship proposed in the literature. Therefore, it will need to be established from a very significant and costly experimental study (different concretes, geometries and percentage of fibers to be considered), or obtained for each specific FRC. In both cases, as with static tests, uniaxial tensile tests on notched specimens will need to be conducted at different loading rates, from low until high loading rates through intermediate loading rates. For the low and intermediate loading rates, a classic traction machine can be used, while for high loading rates the Hopkinson bar is the most effective testing method to be used [24–27].

To enable the experimental determination of the evolution of the uniaxial tensile stress–strain law (Figure 1) – more specifically, the various parameters related to the fibers' bridging effect – with respect to the strain rate for a given FRC, it is essential to assume about this evolution. Referring to chapters 3 and 4, the following assumption appears acceptable:

- The elastic modulus Eb is not a lot of affected by strain rate effects (this Young modulus is mainly linked to the one of the fibers which is not sensitive to the domain of strain rates considered).
- Due to the improvement of fiber anchorage or adhesion to concrete with increasing strain rate, the stress σ1C increases with strain rate.
- Since, even when fibers start to slip within the concrete (descending branch of the bridging effect in Figure 1), few additional microcracks can appear around the fibers (the tensile stresses transmitted near the fibers decrease significantly), the viscous effects associated with this slipping can be neglected.

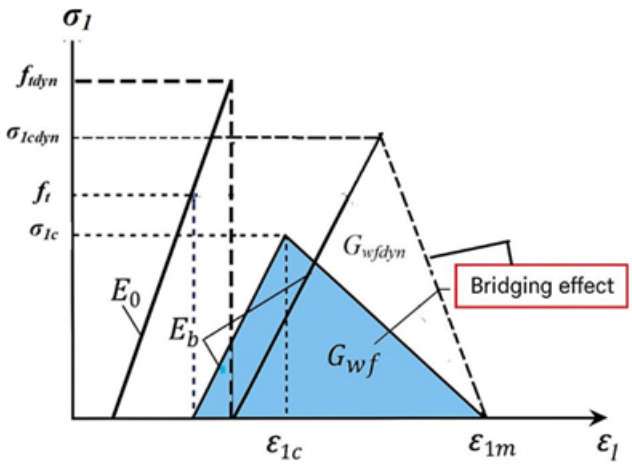

Figure 4: Aspects of the PSEC^f model in dynamics.

- The strain ε_{1m} (Figure 1), mainly related to the fiber's geometry and dimensions, can be assumed to be unaffected (or minimally affected, so no considered) by strain rate effects.

In consequence, the strain rate effects accompanying the proposed fiber bridging effect are primarily related to the enhancement of fiber adhesion or anchorage (increasing of σ_{1c} which becomes σ_{1Cdyn}). Figure 4 summaries the PSEC^f model in dynamics. As previously stated, experimental studies to access the parameters of the proposed model are complex (especially the use of the Hopkinson bar, which is a relatively confidential experimental equipment) and expensive. It is therefore relevant to propose an alternative to these studies by making a few assumptions. Thus, the only value to be determined in the dynamic bridging effect of fibers is that of the parameter (σ_{1Cdyn}). However, as proposed (hypothesis), the value of this parameter is linked to the improvement of the anchoring or adhesion of the fiber in the matrix (depending on the fiber type) with rate effects. Since this improvement is attributable to the Stefan effect on the microcracking process around the fibers and it is a process similar to that which governs the increase in the uniaxial tensile strength of concrete (chapter 2), a new hypothesis can be

put forward: the increase in the value of (σ_{1Cdyn}) with the strain rate follows the same law as that of the tensile strength of concrete. This is reflected in the following relationship (relation (6):

$$\sigma_{1Cdyn} = \sigma_{1Cstat}\left(f_{tdyn}/f_{tsat}\right) \quad (6)$$

From a numerical perspective, the influence of structural inertia should come automatically from a dynamic analysis [28], being a natural consequence of the inclusion of mass matrix and damping matrix in the equation of motion. Therefore, it should not be considered a priori either through Dynamic Increase Factor (DIF) or by sophisticated constitutive models. This choice is supported by thorough numerical simulations [29–31].

It is noteworthy to mention that, at local (finite element) level, structural inertia is only responsible for changing the stress and strain state. Evidently, structural inertia will control whether the finite element will achieve its strength faster or slower, but it will not change its actual value. Concerning the finite element procedure, before starting the numerical analysis, it is necessary to assign random property of f_t and deterministic one of for each finite element according to a given probabilistic distribution concerning ft. This type of procedure was originally de- scribed in [32] for the probabilistic semi-explicit cracking (PSEC) model related to concrete (it means without fibers). Once the probabilistic properties and the deterministic one have been assigned to the finite element mesh, boundary and initial conditions are provided, and a typical dynamic analysis is performed, usually adopting the Newmark-beta algorithm for the time-step integration.

Conclusions and Perspectives

This article presents the fundamentals of a numerical model that is set to undergo subsequent algorithmic implementation. This model is a probabilistic semi-explicit cracking model dedicated to the dynamic behavior of structures made from steel fiber reinforced concrete (SFRC). It is based on the extension of the same model that has been developed and validated in static conditions. This extension is proposed after a detailed exploration of the physical mechanisms accompanying the cracking process of fiber-reinforced concrete under dynamic loading.

The fact that the model is based on precise and detailed physical mechanisms allows for an interesting alternative to the experimental quantification of the model parameters. This experimental quantification, which requires the use of a Hopkinson bar, is complex and costly. The proposed alternative involves conducting only uniaxial tensile tests in static on notched fiber-reinforced concrete specimens. This work provides the scientific and engineering communities with a solid foundation to sup- port such developments. Following this implementation, a validation phase, based on available experimental data from the literature, will be necessary to confirm the accuracy and robustness of this model.

References

1. Rossi P (1994) Dynamic behaviour of concrete: from material to the structure, Materials and Structures 27: 319-323.
2. Rossi P (2023) Basis of Probabilistic Semi-Explicit Cracking Model for Fiber Reinforced Concretes. Cur Trends Civil & Struct Eng 10(1).
3. Rossi P (1988) Les bétons de fibres, Les presses de l'Ecole Nationale des Ponts et Chaussées.
4. Toutlemonde F (1994) Résistance au choc des structures en béton: du comportement du matériau au calcul des ouvrages, PhD thesis, Ecole Nationale des Ponts et Chaussées pp. 394.
5. Fanella D, Krajcinovic D (1985) Continuum damage mechanics of fiber reinforced concrete. J Eng Mech 111(8): 995-1009.
6. Li F, Li Z (2000) Continuum damage mechanics-based modeling of fiber reinforced concrete in tension. Int J Solids Struct 38: 777-793.
7. Peng X, Meyer C (2000) A continuum damage mechanics model for concrete reinforced with randomly distributed short fibers. Comput Struct 78: 505-515.
8. Barros J, Figueiras JA (2001) Model for the analysis of steel fiber reinforced concrete slabs on grade. Computers & Structures 79(1): 97-106.
9. Cunha V, Barros J, Sena-Cruz J (2012) A finite element model with discrete embedded elements for fiber reinforced composites. Computers & Structures 94-95: 22-33.
10. De Montaignac R, Massicotte B, Charron JP (2013) Finite-element modelling of SFRC members in bending. Magazine of Concrete Research 65(19): 1133-1146.
11. Lagier F, Massicotte B, Charron JP (2016) 3D Nonlinear Finite-Element Modeling of Lap Splices in UHPFRC. Journal of Structural Engineering 142(11).
12. MR Rita, P Rossi, E de MR Fairbairn, FLB Ribeiro, JL Tailhan, et al. (2024) 3D probabilistic semi-explicit cracking model for concrete structures. Appl Sci 14(6): 2298.
13. Rossi P (2012) Experimental Study of Scaling Effect Related to Post-Cracking Behaviors of Metal Fibers Reinforced (MFRC). European Journal of Environmental and Civil Engineering 16(10): 1261-1268.
14. Rossi P, Wu X, Le Maou F, Belloc A (1994) Scale effect on concrete in tension. Mater Struct 27: 437–444.
15. Casanova P, Rossi P (1997) Analysis and design of steel fiber reinforced concrete beams. ACI Structural Journal 94(5): 595-602.
16. (2001) RILEM TC 162. Test and design methods for steel fibre reinforced concrete: Uniaxial tension test for steel fibre reinforced concrete. Mater Struct 34(235): 3–6.
17. Hsuan The H, Fu-Ming L, Yih-Yuan J 2004) Nonlinear finite element analysis of reinforced concrete beams strengthened by fiber-reinforced plastics, Composite Structures 63: 71–281.
18. Haido JH, Abu Bakar BH, Jayaprakash J, Abdul Razzak AA (2010) Nonlinear Response of Steel-Fiber Reinforced Concrete Beams under Blast Loading: Material Modeling and Simulation. Ye L, Feng P, Yue Q (eds) Advances in FRP Composites in Civil Engineering. Springer, Berlin, Heidelberg, Germany.
19. Mahdi S, Kolbadi S, Davoodian H, Mohammad S, Kolbadi S (2017) Evaluation of Nonlinear Behavior of Reinforced Concrete Frames by Explosive Dynamic Loading Using Finite Element Method, Civil Engineering Journal 3(12).
20. Arruda MRT, Castro LMS (2021) Non-linear dynamic analysis of reinforced concrete structures with hybrid mixed stress finite elements, Advances in Engineering Software 153: 102965.
21. Shakir HM, Al-Azzawi AA, Al Tameemi AF (2022) Nonlinear Finite element Analysis of Fiber Reinforced Concrete Pavement under Dynamic Loading, Journal of Engineering 28(2).
22. Serdar AH, Caglar N, Demirtas G, Saribiyik M (2024) Nonlinear finite element analysis of steel fiber reinforced concrete beams subjected to impact loads, Revista de la Con- strucción 23(1).
23. Rossi P (2022) Mode I Crack Propagation in Concrete Structures under Impact Loadings, Current Trends in Civil & Structural Engineering.

24. Tong G, Pang J, Tang B, Huang J, Sun J (2025) Experimental study on dynamic mechanical properties of hybrid fiber reinforced concrete at ifferent temperatures, Sci Rep 15: 16149.

25. Khosravani MR, Weinberg K (2018) Construction and Building Materials 190: 1264-1283.

26. Wang Z, Zhou N, Wang J (2012) Using Hopkinson pressure bar to perform dynamic tensile tests on SFRC at medium strain rates, Magazine of Concrete Research 64(8): 657–664.

27. Hassan M, Wille K (2022) Direct tensile behavior of steel fiber reinforced ultra-high performance concrete at high strain rates using modified split Hopkinson tension bar, Composites Part B, 246.

28. L Jin, W Yu, X Du, W Yang (2019) Dynamic size effect of concrete under tension: A numerical study, International Journal of Impact Engineering 132: 103318.

29. Ozbolt, A. Sharma, HW Reinhardt (2011) Dynamic fracture of concrete–compact tension specimen, International J. of solids and structures 48:1534–1543.

30. Ozbolt W Riedel (2013) Modelling the response of concrete structures from strain rate effects to shock induced loading, in: Understanding the Tensile Properties of Concrete, Elsevier, pp. 295– 340.

31. Ozbolt J Bosnjak J, Sola E (2013) Dynamic fracture of concrete compact tension specimen: Experimental and numerical study, International Journal of Solids and Structures 50: 4270–4278.

32. Rita M (2022) Implementation of a macroscopic probabilistic model of cracking concrete using parallelization strategies. PhD Thesis of Federal University of Rio de Janeiro.